

# Screening of Compounds for Identification of Prospective Histone Deacetylase 2 (HDAC 2) Inhibitor: An *In Silico* Molecular Docking, Molecular Dynamics Simulation, and MM-GBSA Approach

Kaushik Kumar Bharadwaj<sup>1</sup>, Iqrar Ahmad<sup>2</sup>, Bijuli Rabha<sup>1</sup>, Tanmay Sarkar<sup>3,\*</sup> , Harun Patel<sup>4</sup>, Arabinda Ghosh<sup>5</sup>, Debabrat Baishya<sup>1,\*</sup>

<sup>1</sup> Department of Bioengineering and Technology, Gauhati University, Guwahati- 781014, Assam, India; kkbhrdwj01@gmail.com (K.K.B.); bijulipep@gmail.com (B.R.); drdbaishya@gmail.com (D.B.);

<sup>2</sup> Department of Pharmaceutical Chemistry, Prof. Ravindra Nikam College of Pharmacy, Gondur, Dhule, 424002, Maharashtra, India; ansariiqrar50@gmail.com;

<sup>3</sup> Department of Food Processing Technology, Malda Polytechnic, West Bengal State Council of Technical Education, Govt. of West Bengal, Malda- 732102 West Bengal, India; tanmays468@gmail.com;

<sup>4</sup> Division of Computer Aided Drug Design, Department of Pharmaceutical Chemistry, R. C. Patel Institute of Pharmaceutical Education and Research, Shirpur, 425405, Maharashtra, India; hpatel\_38@yahoo.com (H.P.);

<sup>5</sup> Department of Computational Biology and Biotechnology, Mahapurasha Srimanta Sankaradeva Viswavidyalaya, Guwahati, Assam- 781032; amalarastar@gmail.com;

\* Correspondence: tanmays468@gmail.com (T.S.); drdbaishya@gmail.com (D.B.);

Received: 6.05.2023; Accepted: 31.12.2023; Published: 5.09.2025

**Abstract:** HDAC 2 overexpression promotes epigenetic silencing of tumor suppressor genes, which leads to cancer. HDAC 2 inhibitors have thus emerged as possible therapeutic approaches against a variety of human malignancies, as they can inhibit the activity of certain HDACs, repair the overexpression of tumor suppressor genes, and induce cell differentiation, cell cycle arrest, and apoptosis. In this study, among 808 virtually screened compounds, Daidzein 7-O-sulfate (PHUB001355) had a significant binding affinity (-8.11 kcal/mol). In Molecular Dynamics simulation (MD) studies for a 100 ns time scale, the compound Daidzein 7-O-sulfate optimizes its conformation and fits in the receptor's active site, justifying the binding affinity. The optimal binding free energy calculations using the Molecular Mechanics Generalized Born Surface Area (MM-GBSA) (-29.603 ± 15.75 kcal/mol) showed the significant role of van der Waals forces and Coulomb interactions in the stability of the respective complex. The pharmacokinetic study showed its potential as a lead compound. The *in-silico* cytotoxicity prediction also confirmed its potential as an active anticancer compound. Therefore, it can be suggested that Daidzein 7-O-sulfate could be a useful bioactive compound as an HDAC 2 inhibitor and could be used in developing epigenetic therapy in cancer to regulate gene expression.

**Keywords:** HDAC 2; molecular docking; ADME; molecular dynamics simulation; MM-GBSA.

© 2025 by the authors. This article is an open-access article distributed under the terms and conditions of the Creative Commons Attribution (CC BY) license (<https://creativecommons.org/licenses/by/4.0/>), which permits unrestricted use, distribution, and reproduction in any medium, provided the original work is properly cited. The authors retain copyright of their work, and no permission is required from the authors or the publisher to reuse or distribute this article, as long as proper attribution is given to the original source.

## 1. Introduction

Epigenetic regulations are considered one of the most important factors in tumor initiation and progression, with acetylation being one of the most widely studied modifications [1]. Histone deacetylases (HDACs) are a family of proteins whose main activity is removing acetyl groups from lysine residues on histone and non-histone substrates, which regulate cell gene transcription [2]. HDAC 2 is proven to be a crucial regulator of many cellular processes, and the discovery and development of HDAC 2 selective inhibitors hold great promise for the treatment of cancer. Furthermore, compared to pan-HDAC inhibitors, specific isoform-selective HDAC inhibitors are said to have a lower incidence of side effects [3]. HDAC 2 is essential for the development of transcription repressor complexes, which control gene expression. Increased deacetylation can prevent tumor-suppressor genes from transcribing, which would otherwise promote cell division, migration, and invasion. Thus, it is often considered a potential target for cancer therapy to inhibit HDAC 2 [4]. As of now, various studies have proved that HDAC 2 has been associated with several cancer types, including breast, pancreatic, colorectal, prostate, lung cancer, melanoma, hematological malignancies, and urothelial cancers, as well as medulloblastoma [5,6]. Because of the overexpression of HDAC 2 in different cancer types, inhibiting it has become a popular emerging therapeutic option for cancer therapeutics. Currently on the market, FDA-approved HDAC inhibitor compounds such as vorinostat (SAHA), romidepsin, chidamide, Belinostat, and Panobinostat are available for cancer therapeutics [7].

Polyphenols present in vegetables, fruits, wine, and tea, such as anthocyanins, stilbenoids, phenolic acids, and flavonoids [8], can interact with epigenetic signaling cascades involved in tumors and metastasis, making them useful in cancer chemoprevention by activating autophagy and protein deacetylation [9].

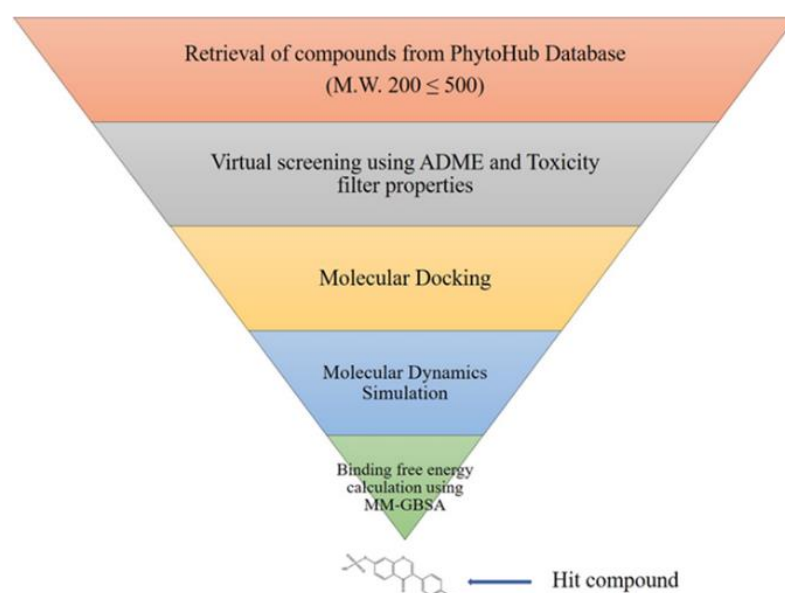


**Figure 1.** Flowchart of the virtual screening workflow for identification of potent HDAC 2 inhibitors from PhytoHub Database compounds.

There are substantial studies that support the use of flavonoids to modulate the epigenome. Flavonoids like quercetin, kaempferol, myricetin, luteolin, apigenin, fisetin, EGCG, genistein, daidzein, silibinin, hesperetin, naringenin, cyanidin, delphinidin, malvidin, and pelargonidin revealed promising preclinical results in epigenetic research [10]. In the

present study, we have employed structure-based virtual screening methods to identify prospective HDAC 2 inhibitors from the PhytoHub database (Figure 1). PhytoHub is a free online database that contains comprehensive information on dietary phytochemicals and their human and animal metabolites. Over 1,200 polyphenols, terpenoids, alkaloids, and other plant secondary metabolites are present in widely consumed foods (>350), as well as >560 human and animal metabolites. We have used various *in silico* methods like drug-likeness prediction, toxicity prediction, molecular docking, MD simulation, MM-GBSA, and cell cytotoxicity prediction calculation to find the prospective HDAC 2 inhibitor.

## 2. Materials and Methods

### 2.1. Preparation of ligands and receptors.

Eight hundred eight (n=808) numbers of compounds from the PhytoHub database (<https://phytohub.eu/>) were used in this study. The Canonical SMILE format of the compounds from the database was retrieved. The compounds were converted to .pdb format using UCSF Chimera (<https://www.cgl.ucsf.edu/chimera/>), and energy minimization was performed [11,12]. The crystal structure of the human HDAC 2 protein was obtained from the protein data bank (PDB) repository ([www.rcsb.org](http://www.rcsb.org)) (PDB ID: 4LY1) with a resolution of 1.57 Å. The water molecules, inhibitors, and other heteroatoms from the protein were removed and used for a molecular docking study.

### 2.2. *In silico* screening of compounds by absorption, distribution, metabolism, excretion, and toxicity (ADMET) prediction.

We have retrieved 808 compounds from the database (<https://phytohub.eu/>), having a molecular weight between 200 and 500 g/mol. Virtual screening of the compounds for drug-like properties was carried out using the free web tool Swiss ADME (<http://www.swissadme.ch/>) [13–17]. The compound selection was based on implementing Lipinski's rule of five: Ghose, Veber, Egan, Muegge, and lead-like properties from the *silico* ADME screening process. The compounds with zero violations were selected in the screening process. Afterward, the selected compounds were further screened for toxicity properties like AMES toxicity, Hepatotoxicity, hERG I and hERG II inhibitors, and skin sensitization properties by using freely accessible web tools pkCSM online web server (<https://biosig.lab.uq.edu.au/pkcsm/prediction>) [18–21]. The screened compounds were further filtered by performing molecular docking using PyRx virtual screening to find the potential hit compound. The compounds showing higher negative binding energy values with HDAC 2 protein were chosen and further docked using Autodock 4.2.6 software for focused docking and accurate docking. The finally obtained compound with the best docking score was further studied by performing a molecular dynamics simulation and an MM-GBSA study.

### 2.3. High-throughput virtual screening using Pyrex molecular docking.

PyRx version 0.8 software (<https://pyrx.sourceforge.io/>), together with Autodock Vina, was used to perform all initial screening of molecules by molecular docking calculations [22–25]. The compound's PDB structures and the macromolecules (HDAC 2) were loaded into PyRx software. During docking, the proteins were considered rigid, whereas the ligands were considered flexible. Different conformations of the ligands were automatically done by

Autodock Vina to best fit the predicted binding site. The docking complexes of the ligands with the corresponding proteins with the highest binding affinity (most negative) were considered and selected.

#### *2.4. Molecular docking using AutoDock 4.2.6.*

For validation of the compounds obtained from PyRx virtual screening, focused molecular docking was carried out using AutoDock 4.2.6 [26–29]. The catalytic site of the HDAC 2 protein was selected as the binding site for molecular docking analysis. The protein structure was kept rigid while keeping the structure of the ligands flexible. Polar hydrogen and Gasteiger charges were added to both the HDAC 2 protein and ligands. AutoDock Tools (v.1.5.6) of the MGL software package were used to prepare PDBQT files of the ligands and proteins. A grid point spacing of 0.500 Å was set, centered on  $x = 21.875$ ,  $y = -18.378$ , and  $z = 0.790$  Å. The output results were saved in the grid parameter file (GPF) format. The Lamarckian genetic algorithm (LGA) approach was employed. The docking procedure was performed by providing the AutoDock executable and PDF files as input, which resulted in the generation of a DLG file. The investigation involved a comprehensive analysis of the binding interactions exhibited by the docking complexes. To gain deeper insights, both 3D and 2D interaction plots were meticulously scrutinized. For interaction analysis, BIOVIA Discovery Studio Visualizer (DSV) Client 2021 (<https://discover.3ds.com/discovery-studio-visualizer-download>) and UCSF Chimera software (<https://www.cgl.ucsf.edu/chimera/>) were used to create the two-dimensional (2D) and three-dimensional (3D) interactions.

#### *2.5. MD simulations.*

The MD simulations were performed for Daidzein 7-O-sulfate (PHUB001355) in a complex with HDAC 2 protein to better understand the dynamic behavior of the targeted protein and the hit compound. The whole MD simulation was run using the Schrodinger Desmond MD simulation program (version 2021-1) [30–33] installed on the Ubuntu 18.04 platform with the Z2 TWR G4 WKS Intel Core i7-9700 and NVIDIA Quadro P620 4GB graphics processing unit. The Daidzein 7-O-sulfate -HDAC 2 complex was solvated in an orthorhombic box shape of the simple point charge (SPC) water model. Additionally, the complex system was neutralized by adding appropriate amounts of counter ions (15 Na<sup>+</sup> and 28 Cl<sup>-</sup>) and keeping the physiological 0.15 M NaCl salt concentrations during the simulation. Minimization was performed using the OPLS-2005 force field to arrange the structure of the protein comfortably inside the simulation boundaries [34–37]. Finally, a constant pressure–constant temperature (NPT) ensemble was used to run the MD simulation at 300.0 K temperature and 1.01325 bar pressure. Long-range electrostatic interactions were calculated using the particle mesh Ewald approach, with the radius for Coulomb interactions set to 9 Å. The bonded forces were calculated using the RESPA integrator with a time step of 2 fs for each trajectory. Using the MD trajectory acquired, the stability and binding orientation of the Daidzein 7-O-sulfate -HDAC 2 complex were studied using the simulation interaction diagram (SID) panel. To check the stability of the MD simulation, the root-mean-square deviation (RMSD), the radius of gyration (Rg), root mean square fluctuation (RMSF), and the number of hydrogen bonds (H-bonds) were computed.

## 2.6. Molecular mechanics generalized born surface area (MM-GBSA) calculations.

The MM-GBSA method is used to compute the relative binding affinity of a Daidzein 7-O-sulfate (in kcal/mol) with the HDAC 2 protein. As a result, the Prime Module's Python script `thermal mmgbsa.py` was utilized to execute post-simulation MM-GBSA analysis. For binding free energy calculations of Daidzein 7-O-sulfate in complex with HDAC 2 protein, 100 ns MD simulation trajectory frames were studied. Individual energy modules such as van der Waals, columbic, covalent, self-contact, solvation, hydrogen bond, lipophilic, and  $\pi$ - $\pi$  stackings of ligand and protein were used collectively to compute the Prime MM-GBSA binding free energy (kcal/mol) [38].

The following formula was used to calculate the total free energy binding:

$$\Delta G_{\text{bind}} = G_{\text{complex}} - (G_{\text{protein}} + G_{\text{ligand}}) \quad (1)$$

Where  $\Delta G_{\text{bind}}$  = binding free energy,  $G_{\text{complex}}$  = free energy of the complex,  $G_{\text{protein}}$  = free energy of the target protein, and  $G_{\text{ligand}}$  = free energy of the ligand.

## 2.7. *In silico* prediction of cytotoxicity for tumor and non-tumor cell lines of the Daidzein 7-O-sulfate.

CLC-Pred (Cell Line Cytotoxicity Predictor) (<http://www.way2drug.com/Cell-line/>), a web-based tool for predicting the cytotoxicity of chemical compounds on human cell lines, was used to predict *in silico* cytotoxicity of the obtained compound against tumor and non-tumor cell lines. The CLC-Pred tool is based on a structure-cell line cytotoxicity relation created using Prediction of Activity Spectra for Substances (PASS) specific training sets with the leave-one-out cross-validation process. The prediction results are around 96% accurate compared to the results of *in vivo* tests [39,40]. The default parameters given in the CLC-protocol Pred were used to interpret the data. "Pa" denotes activity, while "Pi" denotes inactivity. The  $Pa > Pi$  indicates that the likelihood of action is much greater than the likelihood of inaction.

## 3. Results and Discussion

### 3.1. Virtual screening and molecular docking analysis.

Eight hundred eight (n=808) compounds from the database were retrieved. These compounds underwent virtual screening using Swiss ADME, with filters based on properties such as Lipinski, Ghose, Veber, Egan, Muegge, and lead-likeness. The compounds that successfully passed the filters without violating the aforementioned properties were selected. These selected compounds were then subjected to additional screening for toxicity, including AMES toxicity, hepatotoxicity, hERG I and hERG II inhibitors, and skin sensitization properties. Following the toxicity filtering, the compounds were chosen for molecular docking virtual screening utilizing the Autodock Vina PyRx tool. Subsequently, the lead compound with the most favorable binding energy was subjected to additional docking using Autodock 4.2.6 for focused and precise docking. Redocking and cross-docking studies were performed to calculate the most accurate binding energy value [29]. Blind docking by PyRx helped to have the preliminary screening of the compound libraries and suggested that Daidzein 7-O-sulfate interacts with better energy values with the HDAC 2 protein. Next, focused docking was performed by using Autodock, with the HDAC 2 protein and the compound Daidzein 7-

O-sulfate (PHUB001355), which showed a binding energy value of -8.11 kcal/mol with an inhibition constant of 1.14  $\mu$ M. The more negative the docking score value, the higher the binding affinity of the ligand toward the receptor [41]. Previous investigations have conveyed that the compound possessing higher negative binding energy scores obtained after the molecular docking study showed its potential as a potent protein inhibitor in the experimental condition. Compounds like luteolin and apigenin portrayed a more negative docking score value in molecular docking studies against HDAC 2, which was further confirmed in experimental evidence as a potent HDAC inhibitor [11,29]. Our binding energy values are almost similar to previous findings of molecular docking results of the standard drug vorinostat and compounds such as apigenin and luteolin. The binding score of our ligand Daidzein 7-O-sulfate with the HDAC 2 protein was quite significant and comparable to that with potent HDAC 2 inhibitor compound Vorinostat (-8.45 kcal/mol) and flavonoids like luteolin (-9.26 kcal/mol) and apigenin (-9.32 kcal/mol) as reported in the previous finding [11]. Molecular docking interactions of the obtained compound (Daidzein 7-O-sulfate) (Figure 2) with the binding site residues of HDAC 2 are shown in Figure 3. Daidzein 7-O-sulfate interacts with the residues Met 35, Gly 143, Leu 144, His 145, His 146, Gly 154, Phe 155, Cys 156, Asp 181, His 183, Tyr 209, Phe 210, Gln 265, Asp 269, Leu 276, Gly 305, Gly 306, and Tyr 308 in the binding site of HDAC 2 to form the docking complex. The compound Daidzein 7-O-sulfate is able to bind to HDAC 2 by inserting its aromatic rings into the active site pocket with multiple contacts with the amino acid residues at the binding cavity. The compound also showed coordination with  $Zn^{2+}$  of the HDAC 2 protein.  $Zn^{2+}$  ion is the cofactor of HDAC 2 protein and plays an essential role in histone deacetylase activity [42]. The coordination of the compound Daidzein 7-O-sulfate with the cofactor  $Zn^{2+}$  of HDAC 2 showed its binding into the active site binding pocket. The compound Daidzein 7-O-sulfate formed two hydrogen bonds with the amino acid residues Gly 143 and Phe 210. Other than hydrogen bonds, van der Waals,  $\pi$ -sulfur,  $\pi$ -alkyl,  $\pi$ - $\pi$  stacked, and covalent interactions are also formed. Our study corroborates with the previous findings, which also showed that compounds interact with the active site residues of HDAC 2 protein at Phe 155, Asp 181, His 183, Phe 210, Gln 265, Asp 269, Gly 306, and Tyr 308 [11]. To provide virtual, realistic insights into mechanisms and an understanding of inhibition mechanisms, a molecular dynamics simulation is performed [43]. Thus, we perform a deeper analysis to investigate and confirm the better binding stability of the Daidzein 7-O-sulfate -HDAC 2 docked complex further by using molecular dynamics simulation and MM-GBSA study. Flavonoid Daidzein originated from soybean and has been reported to affect the activation and expression of sirtuin (SIRT 1) protein [44,45]. The compound Daidzein 7-O-sulfate ( $C_{15}H_{10}O_7S$ ) (3-(4-hydroxyphenyl)-4-oxo-4H-chromen-7-yl] oxidanesulfonic acid) (PHUB001355) reported in the PhytoHub database has not yet been explored till now as an HDAC 2 inhibitor. The inhibition of HDAC 2 protein by the compound Daidzein 7-O-sulfate showed its potential as an epigenetic modifier. Thereby, this compound can potentially prohibit the proliferation of HDAC 2 protein, overexpressing cancer types such as ovarian, liver, brain, and lung cancer.

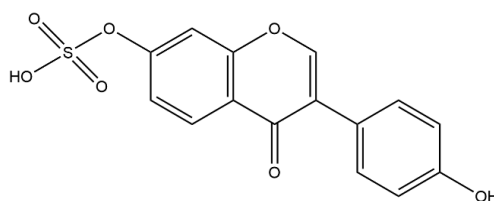


**Figure 2.** Chemical structures of Daidzein 7-O-sulfate (PHUB001355).

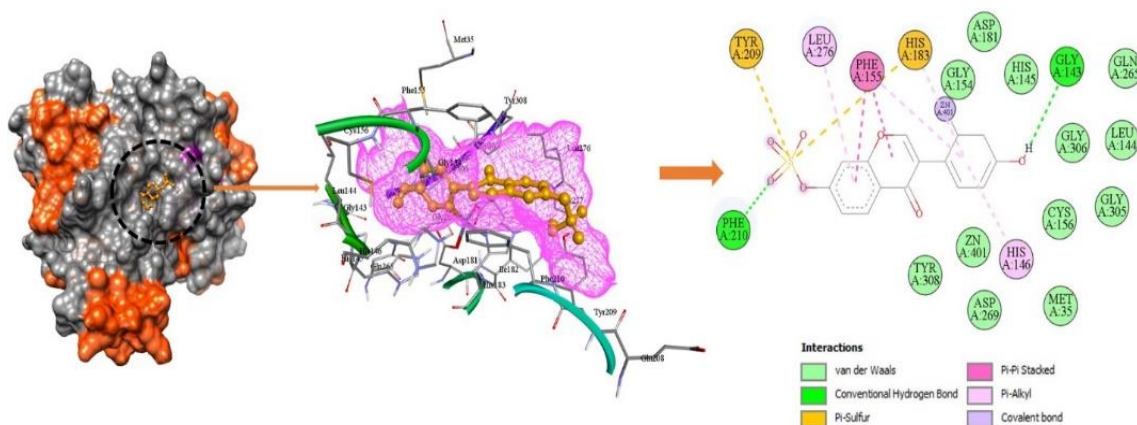


**Figure 3.** Molecular docking interaction of Daidzein 7-O-sulfate (PHUB001355) with HDAC 2 depicting 2D and 3D plots of the ligand interaction with the amino acid residues in the binding site cavity of HDAC 2 protein.

### 3.2. Analysis of (ADMET) studies.

The computed ADMET properties of the compound Daidzein 7-O-sulfate (C<sub>15</sub>H<sub>10</sub>O<sub>7</sub>S) (PHUB001355) are presented in Table 1. According to the result, the compound showed no violation of all five filters (Lipinski, Ghose, Veber, Egan, and Muegge) used. The compound also exhibited lead-like properties, demonstrated high gastrointestinal absorption, and was predicted to have no inhibitory activity against any of the CYP isoforms. The pharmacokinetic and toxicity properties of the compound showed no toxicity. The absence of toxicity is one of the major factors for a compound to be a successful therapeutic candidate. Overall, the ADMET results showed that the compound Daidzein 7-O-sulfate is a potential drug-like compound.

**Table 1.** Predicted ADMET properties of compound Daidzein 7-O-sulfate (C<sub>15</sub>H<sub>10</sub>O<sub>7</sub>S) (PHUB001355) were performed in SwissADME (<http://www.swissadme.ch/>) and the (<https://biosig.lab.uq.edu.au/pkcsm/prediction>) web server.

Properties and functions	Predictive results	
Physicochemical properties	Molecular weight (Da)	334.30 g/mol
	Number of heavy atoms	23
	Number of aromatic heavy atoms	16
	Number of rotatable bonds	3
	Number of H-bond acceptors	7
	Number of H-bond donors	2
	Molar refractivity	82.16
	TPSA	122.42 Å <sup>2</sup>
	Lipophilicity	
	Log Po/w (iLOGP)	1.17
	Log Po/w (XLOGP3)	1.88
	Log Po/w (WLOGP)	3.43
	Log Po/w (MLOGP)	0.52
	Log Po/w (SILICOS-IT)	1.35
	Consensus Log Po/w	1.67
Water solubility	Log S (ESOL)	-3.41
	Solubility	1.29e-01 mg/ml; 3.86e-04 mol/l
	Class	Soluble
	Log S (Ali)	-4.07
	Solubility	2.83e-02 mg/ml; 8.45e-05 mol/l
	Class	Moderately soluble
	Log S (SILICOS-IT)	-4.62
Drug likeness	Solubility	8.11e-03 mg/ml; 2.43e-05 mol/l
	Class	Moderately soluble
Lead likeness	Lipinski, Ghose, Veber, Egan, Muegge	Yes
		Yes
Pharmacokinetics	PAINS	0 alert
	GI absorption	High
	BBB permeant	No

Properties and functions	Predictive results
P-gp substrate	No
CYP1A2 inhibitor	No
CYP2C19 inhibitor	No
CYP2C9 inhibitor	No
CYP2D6 inhibitor	No
CYP3A4 inhibitor	No
Log Kp (skin permeation)	-7.00 cm/s
<b>Toxicity study</b>	
AMES toxicity	No
hERG I inhibitor	No
hERG II inhibitor	No
Hepatotoxicity	No
Skin Sensitisation	No

### 3.3. Molecular dynamics (MD) simulation study.

To explore the stability of the ligand-protein complex and the key intermolecular interactions during the simulated trajectory, the Daidzein 7-O-sulfate docking complex with HDAC 2 protein was exposed to the MD simulation study. The simulated complex trajectories were examined for various standard simulation parameters such as Root mean square deviation (RMSD), Root mean square fluctuations (RMSF), Radius of gyration, and number of hydrogen bond calculations between protein-ligand during 100 ns of MD simulation. Furthermore, the MM-GBSA method was used to calculate Daidzein 7-O-sulfate binding affinity toward the HDAC 2 protein. The C $\alpha$  atoms' RMSD is one of the important parameters of the MD simulation trajectory that is used to investigate the C $\alpha$  structure deviation of a single frame generated in a dynamic environment. Previous research showed that the stability of the protein-ligand complex is determined by the lower RMSD value during the course of the MD simulation. On the other hand, the less stable the protein-ligand complex is, the higher the RMSD value [46]. The C $\alpha$  atoms of the HDAC 2 protein were used to analyze the RMSD, which was then plotted against the simulation time, as presented in Figure 4A. The Daidzein 7-O-sulfate, when bound to HDAC 2, showed RMSD (C $\alpha$  atom of HDAC 2) values between 0.953 Å and 2.601 Å with an average value of 1.98 Å. As can be observed from the results, the complex remained stabilized and stayed that way for the duration of the MD simulation, suggesting that the protein-ligand complex system folded to a stable state. Individual amino acid residues play a critical role in the stability of the protein-ligand complex in the MD simulation study. The RMSF parameter is used to investigate the fluctuation of the residue during the simulation. The RMSF value was assessed from the MD simulation trajectory and is shown in Figure 4B. The RMSF results revealed that the C $\alpha$  of HDAC 2 protein bound to Daidzein 7-O-sulfate has a mean RMSF value of 0.938 Å, indicating fewer fluctuations in the complex structure. However, residues Gly 12 (5.27 Å), Lys 12 (2.918 Å), Gly 30 (2.98 Å), Gln 31 (3.064 Å), Gly 32 (3.2 Å), and His 33 (2.41 Å), Tyr 72 (2.60 Å), Tyr 209 (3.10 Å), Phe 210 (4.36 Å), and Pro 211 (4.23 Å) have shown slight fluctuations in the HDAC 2- Daidzein 7-O-sulfate complex during the 100 ns simulation time. Some amino acid residues fluctuated considerably more than others in the complex. But the overall amino acid residue fluctuation during the interaction was found to be below 2.4, which is satisfactory and acceptable [46]. The binding characteristics of HDAC 2 with ligand Daidzein 7-O-sulfate were analyzed by studying hydrogen bond interactions. The numbers of intermolecular hydrogen bonds during the simulation of the compound with HDAC 2 protein are shown in Figure 4C. Analysis of the results showed that the compound Daidzein 7-O-sulfate formed 2 hydrogen bonds on average during 100 ns of MD simulation time with the HDAC 2. This result confirmed the strong inhibition of HDAC 2 by the compound Daidzein 7-O-sulfate during MD simulation. The study

showed similar interpretations with the molecular docking results of 2 hydrogen bonds within the active site residues in the HDAC 2 protein. The radius of the gyration property was also studied to illustrate the stability of the Daidzein 7-O-sulfate in the HDAC 2 binding pockets during the simulation of 100 ns (Figure 4D). The radius of the gyration parameter is used to calculate how extended a compound is and is equivalent to its principal moment of inertia [46]. The Daidzein 7-O-sulfate in complex with HDAC 2 protein exhibited an average radius of gyration value of 20.24 Å and ranged from 19.83 Å to 20.53 Å. No major fluctuation was observed in the radius of gyration value. These constant values showed steady behavior. Thus, our overall MD simulation results clearly confirmed the advantageous interactions of compound Daidzein 7-O-sulfate with stability in the HDAC 2 active site, depicting the capability as a plausible HDAC 2 inhibitor.

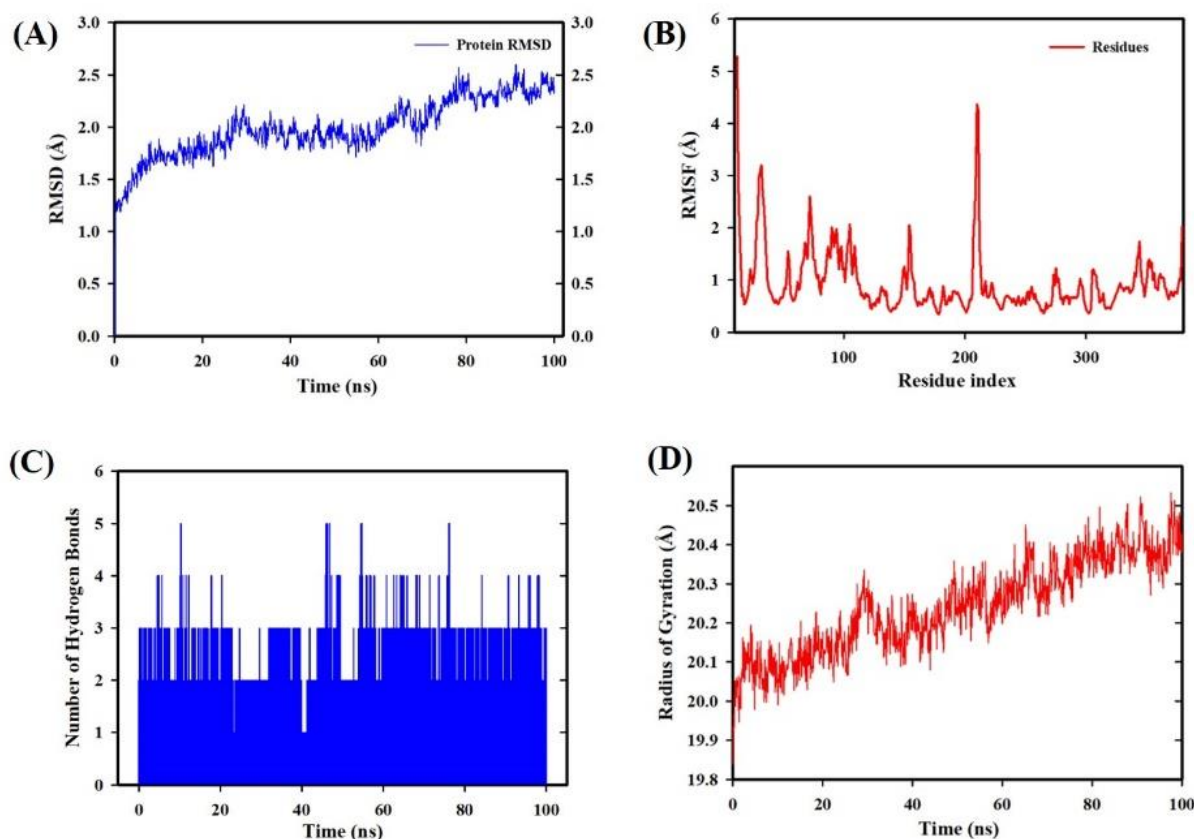


**Figure 4.** MD simulation analysis of Daidzein 7-O-sulfate (PHUB001355) in complex with HDAC 2 during 100 ns MD simulation time (A) Plot of root mean square deviations (RMSD) (C- $\alpha$  atom of HDAC 2 protein); (B) Plot of root mean square fluctuations (RMSF) values; (C) Plot of the number of hydrogen bonding interactions; (D) Plot of Radius of gyration during 100 ns MD simulation time.

#### 3.4. Molecular mechanics generalized born surface area (MM-GBSA) calculations.

Although molecular docking methods are good at predicting the best ligand pose within the protein-binding site, they are not trustworthy enough to rank order compounds based on their binding affinities and, thus, biological activity. This poor correlation could be due to the strong approximations used by docking scoring algorithms, which can significantly amplify errors in such calculations. It has recently been discovered that combining more physically relevant energy parameters like solvation energy and surface accessibility area with a molecular mechanical force field improves the accuracy of ligand binding energy predictions [47]. Thus, the MM-GBSA study was used to perform relatively accurate predictions of compound binding affinity. The computed post-simulation MMGBSA-based binding free

energy for the protein-ligand complex with standard deviation is presented in Table 2. The computed mean  $\Delta G_{\text{Bind}}$  of the complex of Daidzein 7-O-sulfate -HDAC 2 was found to be  $-29.603 \pm 15.75$  kcal/mol. A more negative value shows stronger binding of the compound to the target protein [46]. The results (Table 2) suggested that the maximum contribution to  $\Delta G_{\text{bind}}$  in the stability of the simulated complexes was due to  $\Delta G_{\text{bindvdW}}$  and  $\Delta G_{\text{bindCoulomb}}$ . At the same time,  $\Delta G_{\text{bindCovalent}}$  and  $\Delta G_{\text{bindSolvGB}}$  contributed to the instability of the Daidzein 7-O-sulfate bound HDAC 2 complex.

**Table 2.** Binding free energy components for the docking complexes of HDAC 2 protein with ligand Daidzein 7-O-sulfate, calculated by MM-GBSA analysis.

MM-GBSA (kcal/mol)	Daidzein 7-O-sulfate -HDAC 2
$\Delta G_{\text{bind}}$	$-29.603 \pm 15.75$
$\Delta G_{\text{bindLipo}}$	$-5.671 \pm 2.05$
$\Delta G_{\text{bindvdW}}$	$-29.478 \pm 4.32$
$\Delta G_{\text{bindCoulomb}}$	$-114.821 \pm 18.95$
$\Delta G_{\text{bindHbond}}$	$-2.133 \pm 0.80$
$\Delta G_{\text{bindSolvGB}}$	$123.398 \pm 12.50$
$\Delta G_{\text{bindCovalent}}$	$2.518 \pm 1.94$
$\Delta G_{\text{bind Packing}}$	$-3.415 \pm 2.50$

### 3.5. *In silico* cytotoxicity prediction and analyses.

The cell cytotoxicity of the compound Daidzein 7-O-sulfate on human cell lines was predicted using CLC-Pred: Cell Line Cytotoxicity Predictor (<http://www.way2drug.com/cell-line/>). It is a web-based service for *in silico* prediction of the cytotoxic effects of compounds on non-transformed and cancer cell lines [48]. Out of a maximum likelihood score of 1, the results provide a probability score of activity and inactivity against tumor and non-tumor cells. Small cell lung carcinoma (Lung), Breast carcinoma (Breast), Melanoma (Skin), Adult B acute lymphoblastic leukemia (Leukemia), and Gastric carcinoma (Stomach) for the Daidzein 7-O-sulfate compound had active coefficients of 0.449, 0.398, 0.300, and 0.274, respectively, in the PASS filter, indicating considerable anticarcinogenic action (Table 3). These findings indicate the potential of the Daidzein 7-O-sulfate compound as a promising anticancer agent. Non-tumour cell lines such as Prostate epithelial cell (Prostate), Lymphocyte (HTLV-1 producing cell line) (Blood), and Keratinocyte (skin) exhibited no cytotoxic action with less active coefficients of 0.154, 0.099, and 0.093. These results imply that Daidzein 7-O-sulfate is non-cytotoxic and non-harmful to normal cells.

**Table 3.** Prediction of cell line cytotoxicity of Daidzein 7-O-sulfate (PHUB001355) with tumor and non-tumor cell lines by using CLC-Pred: Cell Line Cytotoxicity Predictor (<http://www.way2drug.com/cell-line/>).

PA*	PI*	Cell line	Cancer type/cell type	Tissue	Tumor type
<b>0.449</b>	0.067	MCF7	Breast carcinoma	Breast	Carcinoma
<b>0.398</b>	0.031	SK-MEL-28	Melanoma	Skin	Melanoma
<b>0.274</b>	0.073	MKN-7	Gastric carcinoma	Stomach	Carcinoma
<b>0.107</b>	0.011	Ishikawa	Endometrial adenocarcinoma	Uterus	Adenocarcinoma
<b>0.102</b>	0.024	Lu1	Lung carcinoma	Lung	Carcinoma
<b>0.103</b>	0.055	COLO 320	Colon adenocarcinoma	Colon	Adenocarcinoma
<b>0.300</b>	0.261	NALM-6	Adult B acute lymphoblastic leukemia	Haematopoietic and lymphoid tissue	Leukemia
<b>0.125</b>	0.094	SH-SY5Y	Bone marrow neuroblastoma	Brain	Neuroblastoma
<b>0.144</b>	0.117	MAXF401	Breast carcinoma	Breast	Carcinoma
<b>0.105</b>	0.083	MeWo	Melanoma	Skin	Melanoma
<b>0.154</b>	0.057	PrEC	Prostate epithelial cell	Prostate	Non-tumour cell line
<b>0.099</b>	0.025	MT2	Lymphocyte (HTLV-1 producing cell line)	Blood	Non-tumour cell line
<b>0.093</b>	0.040	HaCaT	Keratinocyte	Skin	Non-tumour cell line

## 4. Conclusions

According to epigenetic-based cancer therapeutic investigations, histone deacetylase inhibitors induce apoptosis in various cancer cells. HDAC 2 is an epigenetic protein that is overexpressed in tumors such as ovarian, brain, lung, stomach, and colon cancer, and thus a promising target in cancer therapeutics. Our investigation by virtual screening of compounds from the PhytoHub database revealed flavonoid Daidzein 7-O-sulfate as a promising HDAC 2 inhibitor. We have performed various *silico* experiments, such as molecular docking, molecular dynamics simulations, ADMET, and MM-GBSA. Molecular docking, MD simulation, and MM-GBSA analyses indicate that the complex has strong binding affinity, enhanced stability, and greater binding free energy values. The ligand has shown better pharmacokinetic qualities in the ADMET analysis, indicating that it could be a possible lead candidate. The flavonoid Daidzein 7-O-sulfate presented in this study was found to be a suitable HDAC 2 inhibitor. It might play a role in mitigating cancer cell progression by epigenetic chromatin remodeling. Further *in vitro* and *in vivo* research will be needed to validate its anticancer effectiveness precisely. The flavonoid Daidzein 7-O-sulfate presented in this study is proposed as an HDAC 2 inhibitor.

## Author Contributions

All authors have read and agreed to the published version of the manuscript.

## Institutional Review Board Statement

Not applicable.

## Informed Consent Statement

Not applicable.

## Data Availability Statement

Data supporting the findings of this study are available upon reasonable request from the corresponding author.

## Funding

This research received no external funding.

## Acknowledgments

The first author is thankful to MHRD, Govt. of India, for supporting the TEQIP-III fellowship.

## Conflicts of Interest

The authors declare no conflict of interest.

## References

1. Yang, F.; Zhao, N.; Ge, D.; Chen, Y. Next-generation of selective histone deacetylase inhibitors. *RSC Adv.* **2019**, *9*, 19571–19583, <http://doi.org/10.1039/C9RA02985K>.

2. Sixto-López, Y.; Bello, M.; Correa-Basurto, J. Insights into structural features of HDAC1 and its selectivity inhibition elucidated by Molecular dynamic simulation and Molecular Docking. *J. Biomol. Struct. Dyn.* **2019**, *37*, 584–610, <http://doi.org/10.1080/07391102.2018.1441072>.
3. Gediya, P.; Parikh, P.K.; Vyas, V.K.; Ghate, M.D. Histone deacetylase 2: A potential therapeutic target for cancer and neurodegenerative disorders. *Eur. J. Med. Chem.* **2021**, *216*, 113332, <http://doi.org/10.1016/j.ejmech.2021.113332>.
4. Garmpis, N.; Damaskos, C.; Dimitroulis, D.; Kouraklis, G.; Garmpi, A.; Sarantis, P.; Koustas, E.; Patsouras, A.; Psilopatis, I.; Antoniou, E.A.; Karamouzis, M.V.; Kontzoglou, K.; Nonni, A. Clinical Significance of the Histone Deacetylase 2 (HDAC-2) Expression in Human Breast Cancer. *J. Pers. Med.* **2022**, *12*, 1672, <http://doi.org/10.3390/jpm12101672>.
5. Li, Y.; Seto, E. HDACs and HDAC Inhibitors in Cancer Development and Therapy. *Cold Spring Harb. Perspect Med.* **2016**, *6*, <http://doi.org/10.1101/cshperspect.a026831>.
6. Müller, B.M.; Jana, L.; Kasajima, A.; Lehmann, A.; Prinzler, J.; Budczies, J.; Winzer, K.-J.; Dietel, M.; Weichert, W.; Denkert, C. Differential expression of histone deacetylases HDAC1, 2 and 3 in human breast cancer - overexpression of HDAC2 and HDAC3 is associated with clinicopathological indicators of disease progression. *BMC Cancer* **2013**, *13*, 215, <http://doi.org/10.1186/1471-2407-13-215>.
7. Sixto-López, Y.; Gómez-Vidal, J.A.; de Pedro, N.; Bello, M.; Rosales-Hernández, M.C.; Correa-Basurto, J. Hydroxamic acid derivatives as HDAC1, HDAC6 and HDAC8 inhibitors with antiproliferative activity in cancer cell lines. *Sci. Rep.* **2020**, *10*, 10462, <http://doi.org/10.1038/s41598-020-67112-4>.
8. Sarkar, T.; Salaudin, M.; Chakraborty, R. In-depth pharmacological and nutritional properties of bael (*Aegle marmelos*): A critical review. *J. Agric. Food Res.* **2020**, *2*, 100081, <http://doi.org/10.1016/j.jafr.2020.100081>.
9. Ratovitski, E.A. Anticancer Natural Compounds as Epigenetic Modulators of Gene Expression. *Curr. Genomics* **2017**, *18*, 175–205, <http://doi.org/10.2174/1389202917666160803165229>.
10. Khan, H.; Belwal, T.; Efferth, T.; Farooqi, A.A.; Sanches-Silva, A.; Vacca, R.A.; Nabavi, S.F.; Khan, F.; Prasad Devkota, H.; Barreca, D.; Sureda, A.; Tejada, S.; Dacrema, M.; Daglia, M.; Suntar, I.; Xu, S.; Ullah, H.; Battino, M.; Giampieri, F.; Nabavi, S.M. Targeting epigenetics in cancer: therapeutic potential of flavonoids. *Crit. Rev. Food Sci. Nutr.* **2021**, *61*, 1616–1639, <http://doi.org/10.1080/10408398.2020.1763910>.
11. Scafuri, B.; Bontempo, P.; Altucci, L.; De Masi, L.; Facchiano, A. Molecular Docking Simulations on Histone Deacetylases (HDAC)-1 and -2 to Investigate the Flavone Binding. *Biomedicines* **2020**, *8*, 568, <http://doi.org/10.3390/biomedicines8120568>.
12. Pettersen, E.F.; Goddard, T.D.; Huang, C.C.; Couch, G.S.; Greenblatt, D.M.; Meng, E.C.; Ferrin, T.E. UCSF Chimera—A visualization system for exploratory research and analysis. *J. Comput. Chem.* **2004**, *25*, 1605–1612, <http://doi.org/10.1002/jcc.20084>.
13. Daina, A.; Michielin, O.; Zoete, V. SwissADME: a free web tool to evaluate pharmacokinetics, drug-likeness and medicinal chemistry friendliness of small molecules. *Sci. Rep.* **2017**, *7*, 42717, <http://doi.org/10.1038/srep42717>.
14. Ononamadu, C.; Ibrahim, A. Molecular docking and prediction of ADME/drug-likeness properties of potentially active antidiabetic compounds isolated from aqueous-methanol extracts of *Gymnema sylvestre* and *Combretum micranthum*. *BioTechnologia* **2021**, *102*, 85–99, <http://doi.org/10.5114/bta.2021.103765>.
15. Bakchi, B.; Krishna, A.D.; Sreecharan, E.; Ganesh, V.B.J.; Niharika, M.; Maharshi, S.; Puttagunta, S.B.; Sigalapalli, D.K.; Bhandare, R.R.; Shaik, A.B. An overview on applications of SwissADME web tool in the design and development of anticancer, antitubercular and antimicrobial agents: A medicinal chemist's perspective. *J. Mol. Struct.* **2022**, *1259*, 132712, <http://doi.org/10.1016/j.molstruc.2022.132712>.
16. Ayar, A.; Aksahin, M.; Mesci, S.; Yazgan, B.; Gül, M.; Yıldırım, T. Antioxidant, Cytotoxic Activity and Pharmacokinetic Studies by Swiss Adme, Molinspiration, Osiris and DFT of PhTAD-Substituted Dihydropyrrole Derivatives. *Curr. Comput. Aided Drug Des.* **2022**, *18*, 52–63, <http://doi.org/10.2174/1573409917666210223105722>.
17. Joshi, A.A.; Khairnar, S.V.; Chaudhari, H.K. *In silico* ADME/Pharmacokinetic and Target Prediction Studies of Ethambutol as Drug Molecule. *Infect. Disord. Drug Targets* **2022**, *22*, e050122199979, <http://doi.org/10.2174/1871526522666220105113357>.
18. Daoui, O.; Mazoir, N.; Bakhouch, M.; Salah, M.; Benharref, A.; Gonzalez-Coloma, A.; Elkhatabi, S.; El Yazidi, M.; Chtita, S. 3D-QSAR, ADME-Tox, and molecular docking of semisynthetic triterpene derivatives as antibacterial and insecticide agents. *Struct. Chem.* **2022**, *33*, 1063–1084, <http://doi.org/10.1007/s11224-022-01912-4>.

19. Chodankar, R.; Mahajan, A. Characterization and in-silico toxicity prediction of the oxidative degradation products of Pimozide. *Sep. Sci. Plus* **2022**, *5*, 275–284, <http://doi.org/10.1002/sscp.202100065>.
20. Marahatha, R.; Shrestha, A.; Sharma, K.; Regmi, B.P.; Sharma, K.R.; Poudel, P.; Basnyat, R.C.; Parajuli, N. *In Silico* Study of Alkaloids: Neferine and Berbamine Potentially Inhibit the SARS-CoV-2 RNA-Dependent RNA Polymerase. *J. Chem.* **2022**, *2022*, 7548802, <http://doi.org/10.1155/2022/7548802>.
21. Mahmud, S.; Afrose, S.; Biswas, S.; Nagata, A.; Paul, G.K.; Mita, M.A.; Hasan, R.; Shimu, S.S.; Zaman, S.; Uddin, S.; Islam, S.; Saleh, A. Plant-derived compounds effectively inhibit the main protease of SARS-CoV-2: An in silico approach. *PLoS ONE* **2022**, *17*, e0273341, <http://doi.org/10.1371/journal.pone.0273341>.
22. Bhatt, P.; Joshi, T.; Bhatt, K.; Zhang, W.; Huang, Y.; Chen, S. Binding interaction of glyphosate with glyphosate oxidoreductase and C–P lyase: Molecular docking and molecular dynamics simulation studies. *J. Hazard. Mater.* **2021**, *409*, 124927, <http://doi.org/10.1016/j.jhazmat.2020.124927>.
23. Perike, N.; Edigi, P.K.; Nirmala, G.; Thumma, V.; Bujji, S.; Naikal, P.S. Synthesis, Anticancer Activity and Molecular Docking Studies of Hybrid Molecules Containing Indole-Thiazolidinedione-Triazole Moieties. *ChemistrySelect* **2022**, *7*, e202203778, <http://doi.org/10.1002/slct.202203778>.
24. Veerasamy, R.; Karunakaran, R. Molecular docking unveils the potential of andrographolide derivatives against COVID-19: an in silico approach. *J. Genet. Eng. Biotechnol.* **2022**, *20*, 58, <http://doi.org/10.1186/s43141-022-00339-y>.
25. Saravanan, R.; Raja, K.; Shanthi, D. GC–MS Analysis, Molecular Docking and Pharmacokinetic Properties of Phytocompounds from *Solanum torvum* Unripe Fruits and Its Effect on Breast Cancer Target Protein. *Appl. Biochem. Biotechnol.* **2022**, *194*, 529–555, <http://doi.org/10.1007/s12010-021-03698-3>.
26. Forli, S.; Huey, R.; Pique, M.E.; Sanner, M.F.; Goodsell, D.S.; Olson, A.J. Computational protein–ligand docking and virtual drug screening with the AutoDock suite. *Nat. Protoc.* **2016**, *11*, 905–919, <http://doi.org/10.1038/nprot.2016.051>.
27. Morris, G.M.; Huey, R.; Lindstrom, W.; Sanner, M.F.; Belew, R.K.; Goodsell, D.S.; Olson, A.J. AutoDock4 and AutoDockTools4: Automated docking with selective receptor flexibility. *J. Comput. Chem.* **2009**, *30*, 2785–2791, <http://doi.org/10.1002/jcc.21256>.
28. Geethapriya, J.; Shanthidevi, A.; Arivazhagan, M.; Elangovan, N.; Thomas, R. Synthesis, structural, DFT, quantum chemical modeling and molecular docking studies of (E)-4-(((5-methylfuran-2-yl)methylene)amino) benzenesulfonamide from 5-methyl-2-furaldehyde and sulfanilamide. *J. Indian Chem. Soc.* **2022**, *99*, 100418, <http://doi.org/10.1016/j.jics.2022.100418>.
29. Bülbül, E.F.; Melesina, J.; Ibrahim, H.S.; Abdelsalam, M.; Vecchio, A.; Robaa, D.; Zessin, M.; Schutkowski, M.; Sippl, W. Docking, Binding Free Energy Calculations and In Vitro Characterization of Pyrazine Linked 2-Aminobenzamides as Novel Class I Histone Deacetylase (HDAC) Inhibitors. *Molecules* **2022**, *27*, 2526, <http://doi.org/10.3390/molecules27082526>.
30. AbdElmoniem, N.; H. Abdallah, M.; M. Mukhtar, R.; Moutasim, F.; Rafie Ahmed, A.; Edris, A.; Ibraheem, W.; Makki, A.A.; M. Elshamly, E.; Elhag, R.; Osman, W.; Mothana, R.A.; Alzain, A.A. Identification of Novel Natural Dual HDAC and Hsp90 Inhibitors for Metastatic TNBC Using E-Pharmacophore Modeling, Molecular Docking, and Molecular Dynamics Studies. *Molecules* **2023**, *28*, 1771, <http://doi.org/10.3390/molecules28041771>.
31. Mishra, A.; Singh, A. Discovery of Histone Deacetylase Inhibitor Using Molecular Modeling and Free Energy Calculations. *ACS Omega* **2022**, *7*, 18786–18794, <http://doi.org/10.1021/acsomega.2c01572>.
32. Bharadwaj, K.K.; Ahmad, I.; Pati, S.; Ghosh, A.; Sarkar, T.; Rabha, B.; Patel, H.; Baishya, D.; Edinur, H.A.; Abdul Kari, Z.; Ahmad Mohd Zain, MR; Rosli, WIW Potent Bioactive Compounds From Seaweed Waste to Combat Cancer Through Bioinformatics Investigation. *Front. Nutr.* **2022**, *9*, 889276, <http://doi.org/10.3389/fnut.2022.889276>.
33. Kumar, S.; Manoharan, A.; J, J.; Abdelgawad, M.A.; Mahdi, W.A.; Alshehri, S.; Ghoneim, M.M.; Pappachen, L.K.; Zachariah, S.M.; Aneesh, TP; Mathew, B. Exploiting butyrylcholinesterase inhibitors through a combined 3-D pharmacophore modeling, QSAR, molecular docking, and molecular dynamics investigation. *RSC Adv.* **2023**, *13*, 9513–9529, <http://doi.org/10.1039/D3RA00526G>.
34. Bowers, K.J.; Chow, D.E.; Xu, H.; Dror, R.O.; Eastwood, M.P.; Gregersen, B.A.; Klepeis, J.L.; Kolossvary, I.; Moraes, M.A.; Sacerdoti, F.D.; Salmon, J.K.; Shan, Y.; Shaw, D.E. Scalable Algorithms for Molecular Dynamics Simulations on Commodity Clusters. Proceedings of the 2006 ACM/IEEE Conference on Supercomputing - SC '06; Tampa, FL, USA, 11-17 November 2006, ACM Press: New York, New York, USA, **2006**, 84, <http://doi.org/10.1109/SC.2006.54>.

35. Chow, E.; Rendleman, C.A.; Bowers, K.J.; Dror, R.O.; Hughes, D.H.; Gullingsrud, J.; Sacerdoti, F.D.; Shaw, D.E. Desmond Performance on a Cluster of Multicore Processors. **2008**.
36. Shivakumar, D.; Williams, J.; Wu, Y.; Damm, W.; Shelley, J.; Sherman, W. Prediction of Absolute Solvation Free Energies Using Molecular Dynamics Free Energy Perturbation and the OPLS Force Field. *J. Chem. Theory Comput.* **2010**, *6*, 1509–1519, <http://doi.org/10.1021/ct900587b>.
37. Jorgensen, W.L.; Chandrasekhar, J.; Madura, J.D.; Impey, RW; Klein, M.L. Comparison of simple potential functions for simulating liquid water. *J. Chem. Phys.* **1983**, *79*, 926–935, <http://doi.org/10.1063/1.445869>.
38. Bharadwaj, K.K.; Sarkar, T.; Ghosh, A.; Baishya, D.; Rabha, B.; Panda, MK; Nelson, B.R.; John, A.B.; Sheikh, H.I.; Dash, B.P.; Edinur, H.A.; Pati, S. Macrolactin A as a Novel Inhibitory Agent for SARS-CoV-2 M<sup>pro</sup>: Bioinformatics Approach. *Appl. Biochem. Biotechnol.* **2021**, *193*, 3371–3394, <http://doi.org/10.1007/s12010-021-03608-7>.
39. Lagunin, A.A.; Dubovskaja, V.I.; Rudik, A.V.; Pogodin, P.V.; Druzhilovskiy, D.S.; Glorizova, T.A.; Filimonov, D.A.; Sastry, N.G.; Poroikov, V.V. CLC-Pred: A freely available web-service for in silico prediction of human cell line cytotoxicity for drug-like compounds. *PLoS ONE* **2018**, *13*, e0191838, <http://doi.org/10.1371/journal.pone.0191838>.
40. Chinnasamy, P.; Arumugam, R. *In silico* prediction of anticarcinogenic bioactivities of traditional anti-inflammatory plants used by tribal healers in Sathyamangalam wildlife Sanctuary, India. *Egypt. J. Basic Appl. Physiol.* **2018**, *5*, 265–279, <http://doi.org/10.1016/j.ejbas.2018.10.002>.
41. Sarkar, T.; Bharadwaj, K.K.; Salaudinn, M.; Pati, S.; Chakraborty, R. Phytochemical Characterization, Antioxidant, Anti-Inflammatory, Anti-Diabetic Properties, Molecular Docking, Pharmacokinetic Profiling, and Network Pharmacology Analysis of the Major Phytoconstituents of Raw and Differently Dried *Mangifera Indica* (Himsagar Cultivar): An In Vitro and In Silico Investigations. *Appl. Biochem. Biotechnol.* **2022**, *194*, 950–987, <http://doi.org/10.1007/s12010-021-03669-8>.
42. Zhang, L.; Zhang, J.; Jiang, Q.; Zhang, L.; Song, W. Zinc binding groups for histone deacetylase inhibitors. *J. Enzyme Inhib. Med. Chem.* **2018**, *33*, 714–721, <http://doi.org/10.1080/14756366.2017.1417274>.
43. Zhou, H.; Wang, C.; Ye, J.; Chen, H.; Tao, R. Design, virtual screening, molecular docking and molecular dynamics studies of novel urushiol derivatives as potential HDAC2 selective inhibitors. *Gene* **2017**, *637*, 63–71, <http://doi.org/10.1016/j.gene.2017.09.034>.
44. Seidel, C.; Schnekenburger, M.; Dicato, M.; Diederich, M. Histone deacetylase modulators provided by Mother Nature. *Genes Nutr.* **2012**, *7*, 357–367, <http://doi.org/10.1007/s12263-012-0283-9>.
45. Rasbach, K.A.; Schnellmann, R.G. Isoflavones Promote Mitochondrial Biogenesis. *J. Pharmacol. Exp. Ther.* **2008**, *325*, 536–543, <http://doi.org/10.1124/jpet.107.134882>.
46. Zrieq, R.; Ahmad, I.; Snoussi, M.; Noumi, E.; Iriti, M.; Algahtani, F.D.; Patel, H.; Saeed, M.; Tasleem, M.; Sulaiman, S.; Aouadi, K.; Kadri, A. Tomatidine and Patchouli Alcohol as Inhibitors of SARS-CoV-2 Enzymes (3CL<sup>pro</sup>, PL<sup>pro</sup> and NSP15) by Molecular Docking and Molecular Dynamics Simulations. *Int. J. Mol. Sci.* **2021**, *22*, 10693, <http://doi.org/10.3390/ijms221910693>.
47. Sirous, H.; Campiani, G.; Calderone, V.; Brogi, S. Discovery of novel hit compounds as potential HDAC1 inhibitors: The case of ligand- and structure-based virtual screening. *Comput. Biol. Med.* **2021**, *137*, 104808, <http://doi.org/10.1016/j.compbimed.2021.104808>.
48. Yusuf, M.; Khan, S.A. Assessment of ADME and *in silico* Characteristics of Natural-Drugs from Turmeric to Evaluate Significant COX2 Inhibition. *Biointerface Res. Appl. Chem.* **2023**, *13*, 5, <http://doi.org/10.33263/BRIAC131.005>.

## Publisher's Note & Disclaimer

The statements, opinions, and data presented in this publication are solely those of the individual author(s) and contributor(s) and do not necessarily reflect the views of the publisher and/or the editor(s). The publisher and/or the editor(s) disclaim any responsibility for the accuracy, completeness, or reliability of the content. Neither the publisher nor the editor(s) assume any legal liability for any errors, omissions, or consequences arising from the use of the information presented in this publication. Furthermore, the publisher and/or the editor(s) disclaim any liability for any injury, damage, or loss to persons or property that may result from the use of any ideas, methods, instructions, or products mentioned in the content. Readers are encouraged to independently verify any information before relying on it, and the publisher assumes no responsibility for any consequences arising from the use of materials contained in this publication.